general, a gate will be placed in parallel with the load, which will often consist of the grid of another element. Assume that a current just less than I_c flows through the superconducting gate. The grid is then activated with a current I_1 (much less than I_c) which produces a resistance $R(I_c,I_1)$ in the gate. Current will be deflected to the superconducting load of inductance L and will reach a magnitude I_1 in a time

$$\tau \approx L/Rg' \tag{4}$$

where $g'=I_c/I_1$. In practice, the inductance of interconnections can be made negligible by strip-line techniques so that to obtain a figure for the time constant it is appropriate to put L as the inductance of one grid. The calculated value of L is $4.10^{-9}H$ for a grid 15 μ wide and 0.33 cm long. Substituting from the data of Fig. 2 in (4) gives the effective time constant of the experimental device as $\tau \approx 20$ μsec for $I_1=40$ ma. This figure has been confirmed experimentally in circuits which involve elements driving each other.

It is anticipated that the provision of a superconducting shield plane close to the grid itself, reducing its inductance, will raise the operating speed by an order of magnitude. This has been confirmed by an experiment which yielded a time constant of less than 3 μsec.

It has been established that the magnetic interaction between transverse superconducting films is in agreement with the results of a simple calculation. This result can be applied to the construction of complex electronic circuits where both the active and connective elements can be laid down by a process consisting of a small number of steps.

Furthermore, the crossed-strip superconductive element makes practicable the construction of nondestructive readout "catalog" memory systems[3] which will vastly increase the performance capabilities of digital computers.

* A portion of this research was supported in part by the U. S. Atomic Energy Commission, under a letter contract.

[1] D. A. Buck, Proc. Inst. Radio Engrs. **44**, 482 (1956).
[2] J. W. Bremer and V. L. Newhouse, Bull. Am. Phys. Soc. Ser. II, **4**, 225 (1959).
[3] A. E. Slade and H. O. McMahon, Proc. East. Jt. Compt. Conf., Am. Inst. Elec. Engrs. New York, 1956, p. 115.

Silvered Ruby Maser Cavity*

LLOYD G. CROSS
The University of Michigan, Willow Run Laboratories, Ann Arbor, Michigan
(Received May 11, 1959)

SHORTLY after ruby was proposed as a maser material,[1] it occurred to us that the metal bonding properties of ruby could be utilized to prepare silver-coated ruby maser cavities. Since then we have constructed several X-band cavity masers using rectangular parallelepipeds of ruby coated with a thin layer of metallic silver as the maser cavity. Figure 1 is a photograph of 3 typical cavities.

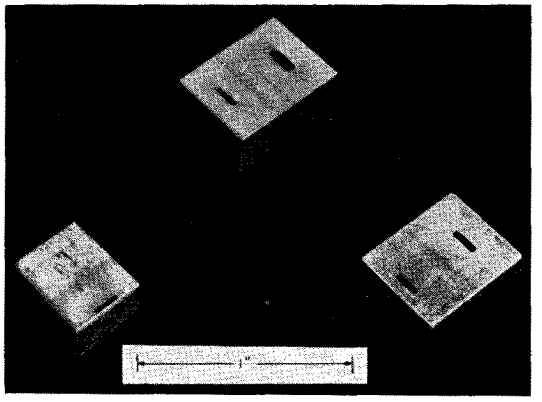

FIG. 1. X-Band silvered ruby cavities.

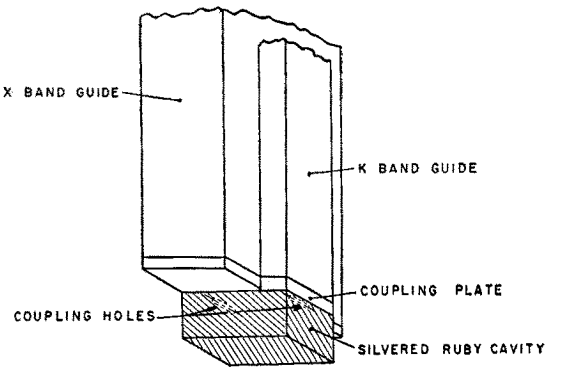

FIG. 2. X-Band maser assembly using silvered ruby cavity.

The silvering procedure is quite simple and requires little preparation. After the ruby is cut and ground to the desired cavity dimensions, it is washed in acetone and a very thin coat of silver paint (Hanovia No. 32-A) is applied to the surfaces. The sample is then baked at 700°C for approximately 30 min. Two more coats are applied as before and the treatment is completed. This procedure was suggested by the work done on lavite cavities in this laboratory.[2]

To provide the microwave coupling to the cavity, slots are cut in the silvering with a dust cutter. The dust cutter provides a thin stream of forced air carrying Al_2O_3 dust which removes the silvering quickly and accurately without cutting the ruby. Using this procedure the coupling slots may be cut to any desired geometry, and if a change is required, the slots can be resilvered and cut again.

The resulting loss "Q" for a silvered ruby cavity is very close to the calculated maximum. In a particular case of a cavity of dimensions $0.68\times0.5\times0.45$ in. the loss "Q" for the TM-112 mode was observed to be approximately 4000. Since the loss tangent of ruby is given as 0.0002, the limiting "Q" due to dielectric losses alone is 5000. The silver coating will not flake or chip off and can be scraped off only with difficulty. Repeated temperature cycling from 300 to 4.2°K has shown no observable effect on any of the cavities.

A practical advantage of the silvered ruby cavity over the ordinary machined cavity is the considerable saving in machining time and expense, especially when the cavity design is in the experimental stage. It is also inherently more stable and less lossy than the ordinary metal cavity. These cavities may be soldered to a wave-guide structure in the manner shown in Fig. 2, or, to allow for more versatility, simply clamped to the coupling plate. In this manner several cavities covering a range of frequencies can be used interchangeably with a single wave-guide structure.

The author wishes to acknowledge the encouragement of R. W. Terhune and J. Lambe during the progress of this work.

* This research was supported by Project Michigan (administered by the U. S. Army Signal Corps).
[1] Makhov, Kikuchi, Lambe, and Terhune, Phys. Rev. **109**, 1399 (1958).
[2] J. Lambe and R. Ager, Rev. Sci. Instr. (submitted for publication).

Forced Magnetostriction of Nickel

R. C. HALL
Magnetic Materials Development Section, Westinghouse Electric Corporation, East Pittsburgh, Pennsylvania
(Received April 24, 1959)

IN a recent review of magnetostriction, Carr[1] noted discrepancies in the published values of volume or isotropic forced magnetostriction for nickel. Strain gauge measurements on poly-

crystalline material by Azumi and Goldman[2] and Bitler[3] indicated values of about -0.55×10^{-10} oe^{-1} for $\partial\omega/\partial H$ or the volume magnetostriction. On the other hand, by other methods of measurement on polycrystalline nickel, Snoek,[4] Kornetzki,[5] Döring,[6] Ebert and Kussmann,[7] Jones and Stacey,[8] and Klitzing and Gielessen[9] have taken data generally indicating values of about 1×10^{-10} to 2×10^{-10} oe^{-1} for $\partial\omega/\partial H$, and in some cases greater.

Recent strain gauge measurements of the magnetostriction of a single crystal of nickel[10] yielded data from which the volume magnetostriction can be calculated. This note gives for the nickel single crystal the values of isotropic and anisotropic forced magnetostriction derived as previously reported.[11] Values of forced magnetostriction (that strain resulting from the application of high fields above "saturation") were taken between field strengths of 5000 and 10 000 oe. The forced magnetostriction was corrected for the lack of true saturation in the single crystal and for the magnetoresistance effect of the strain gauges. The corrected forced magnetostriction was analyzed for isotropic and anisotropic components as previously described.[11]

For the isotropic forced or volume magnetostriction of nickel

$$\partial\omega/\partial H=3\times10^{-10}\text{ oe}^{-1}.$$

This value was estimated to be accurate within 30 or 40% and would indicate that $\partial\omega/\partial H$ for nickel is positive. The two anisotropic forced magnetostriction constants were $h_1'=-0.5\times10^{-10}$ oe^{-1} and $h_2'=0.6\times10^{-10}$ oe^{-1}. These values, the first reported for nickel, are estimated to be accurate within about 50%. They indicate that the anisotropic component of the forced magnetostriction is small.

The author appreciates the help of W. J. Carr for bringing this problem to his attention and for discussions concerning it.

[1] W. J. Carr, Am. Soc. Metals Seminar, Cleveland, Ohio, October 26, 1958.
[2] K. Azumi and J. E. Goldman, Phys. Rev. **93**, 630 (1954).
[3] W. R. Bitler, thesis, Carnegie Institute of Technology (1958).
[4] J. L. Snoek, Physica **4**, 853 (1937).
[5] M. Kornetzki, Z. Physik **97**, 662 (1935).
[6] W. Döring, Z. Physik **103**, 560 (1936).
[7] H. Ebert and A. Kussmann, Physik. Z. **38**, 437 (1937).
[8] G. O. Jones and F. D. Stacey, Proc. Phys. Soc. (London) **B66**, 255 (1953).
[9] K. H. v. Klitzing and J. Gielessen, Z. Physik **146**, 59 (1956).
[10] R. C. Hall, J. Appl. Phys. **30**, 816 (1959).
[11] R. C. Hall, J. Appl. Phys. **28**, 707 (1957).

Perturbation of Wave Guides and Cavities by Spheres and Cylinders*

W. Hauser and L. Brown
Lincoln Laboratory, Massachusetts Institute of Technology, Lexington, Massachusetts
(Received March 11, 1959)

We have utilized an integral equation technique in order to obtain a first-order estimate of the effect of the presence of a plane wall on the electromagnetic fields within a cylinder or sphere a short distance d from a wall. This information is important as it yields an estimate of the best accuracy one can expect to obtain from a free space calculation such as Hurd's[1] in cavity and wave-guide problems.

In the problem of the perturbation of a wave guide or cavity by an obstacle, the quantity of interest is given by a formula of the form[2]

$$\text{quantity of interest}=\int\mathbf{E}_0^*\cdot\boldsymbol{\varepsilon}'\cdot\mathbf{E}d\tau+\int\mathbf{H}_0^*\cdot\boldsymbol{\mu}'\cdot\mathbf{H}d\tau \quad (1)$$

involving the unperturbed fields $\mathbf{E}_0$, $\mathbf{H}_0$, and the actual fields $\mathbf{E}$ and $\mathbf{H}$ within the obstacle.

For first-order results it is customary[3] to neglect the effect of the walls of the guide or cavity and to find the fields from a free space calculation. The integral equations for the electromagnetic field in a free space calculation are

$$\mathbf{E}(\mathbf{r}')=\mathbf{E}_0(\mathbf{r}')+\omega^2\mu_0\int\boldsymbol{\Gamma}^0(\mathbf{r}'|\mathbf{r})\cdot\boldsymbol{\varepsilon}'\cdot\mathbf{E}(\mathbf{r})d\tau$$
$$-j\omega\int\{\nabla\times\boldsymbol{\Gamma}^0(\mathbf{r}|\mathbf{r}')\}^T\cdot\boldsymbol{\mu}'\cdot\mathbf{H}(\mathbf{r})d\tau \quad (2a)$$

and

$$\mathbf{H}(\mathbf{r}')=\mathbf{H}_0(\mathbf{r}')+\omega^2\epsilon_0\int\boldsymbol{\Gamma}^0(\mathbf{r}'|\mathbf{r})\cdot\boldsymbol{\mu}'\cdot\mathbf{H}(\mathbf{r})d\tau$$
$$+j\omega\int[\nabla\times\boldsymbol{\Gamma}^0(\mathbf{r}|\mathbf{r}')]^T\cdot\boldsymbol{\varepsilon}'\cdot\mathbf{E}(\mathbf{r})d\tau \quad (2b)$$

where $\boldsymbol{\Gamma}^0(\mathbf{r}|\mathbf{r}')$ is the free space dyadic Green's function.[4]

If we include the wall, we obtain the integral equations

$$\mathbf{E}(\mathbf{r}')=\mathbf{E}_0(\mathbf{r}')+\omega^2\mu_0\int\boldsymbol{\Gamma}^{(1)}(\mathbf{r}'|\mathbf{r})\cdot\boldsymbol{\varepsilon}'\cdot\mathbf{E}(\mathbf{r})d\tau$$
$$-j\omega\int\nabla'\times\boldsymbol{\Gamma}^2(\mathbf{r}'|\mathbf{r})\cdot\boldsymbol{\mu}'\cdot\mathbf{H}(\mathbf{r})d\tau$$

and (3)

$$\mathbf{H}(\mathbf{r}')=\mathbf{H}_0(\mathbf{r}')+\omega^2\epsilon_0\int\boldsymbol{\Gamma}^2(\mathbf{r}'|\mathbf{r})\cdot\boldsymbol{\mu}'\cdot\mathbf{H}(\mathbf{r})d\tau$$
$$+j\omega\int\nabla'\times\boldsymbol{\Gamma}^{(1)}(\mathbf{r}'|\mathbf{r})\cdot\boldsymbol{\varepsilon}'\cdot\mathbf{E}(\mathbf{r})d\tau$$

where $\boldsymbol{\Gamma}^{(1)}$ and $\boldsymbol{\Gamma}^{(2)}$ are, respectively, the electric and magnetic dyadic Green's functions for the problem.[4] The difference between Eqs. (2) and (3),

$$\Delta E(\mathbf{r}')=\omega^2\mu_0\int\boldsymbol{\Gamma}_-(\mathbf{r}'|\mathbf{r})\cdot\boldsymbol{\varepsilon}'\cdot\mathbf{E}(\mathbf{r})d\tau$$
$$-j\omega\int\nabla'\times\boldsymbol{\Gamma}_+(\mathbf{r}'|\mathbf{r})\cdot\boldsymbol{\mu}'\cdot\mathbf{H}(\mathbf{r})d\tau$$

and (4)

$$\Delta\mathbf{H}(\mathbf{r}')=\omega^2\epsilon_0\int\boldsymbol{\Gamma}_+(\mathbf{r}'|\mathbf{r})\cdot\boldsymbol{\mu}'\cdot\mathbf{H}(\mathbf{r})d\tau$$
$$+j\omega\int\nabla'\times\boldsymbol{\Gamma}_-(\mathbf{r}'|\mathbf{r})\cdot\boldsymbol{\varepsilon}'\cdot\mathbf{E}(\mathbf{r})d\tau,$$

thus represent the contribution of the wall to the fields.

$$\boldsymbol{\Gamma}_-=\boldsymbol{\Gamma}^{(1)}-\boldsymbol{\Gamma}^0 \quad\text{and}\quad \boldsymbol{\Gamma}_+=\boldsymbol{\Gamma}^{(2)}-\boldsymbol{\Gamma}^{(0)}.$$

Utilizing the quasi-stationary approximation of uniform fields within the obstacle, we have obtained a first-order estimate of the contribution of the wall on the fields within the obstacle.

For the case of a thin cylinder a distance $d\sim1/k$ from the wall these contributions are of order $(ka)^2$ and higher, where a is the radius of the cylinder, while for a sphere these contributions are of order $(ka)^3$ and higher. It would be meaningless therefore to carry the free space calculations to any higher order than the above for each case.

Assuming a Taylor expansion of the fields within the obstacle of the form

$$\mathbf{A}+k\mathbf{B}\cdot\mathbf{r}+\cdots$$

where $\mathbf{A}$ is a constant vector and $\mathbf{B}$ a constant dyadic we find that

$$\mathbf{A}=\mathbf{A}_0+\mathbf{A}_1(ka)^2+0(k^3a^3) \quad (5)$$

and

$$\mathbf{B}=\mathbf{B}_0+0(k^2a^2).$$

For cylindrical obstacles, since the term $k\mathbf{B}\cdot\mathbf{r}$ contributes terms of order $(ka)^2$ and higher when inserted into Eq. (1), we need but consider the term $\mathbf{A}_0$ in the Taylor expansion of the fields within the cylinder in a free space calculation.

For spherical obstacles we can include the terms $\mathbf{A}_1(ka)^2$ and $\mathbf{B}_0$.

We have obtained a first-order estimate of the effect of a plane wall and the effect of size on the apparent susceptibility of a ferrite sphere. Our result for the size effect agrees with the result obtained by Hurd.[1]

For a ferrite sphere situated at a point of zero electric field having the dc and rf magnetic fields parallel to the wall and perpendicular to each other,

$$(\mu_{\text{eff}}')=\frac{\chi_+}{2}\left[\frac{1+(\alpha\chi_+/2)}{1+\frac{1}{3}\chi_++\frac{3}{2}\alpha\chi_+}\right] \quad (6)$$

where $\chi_+=4\pi M/(H_0-H-jH_1)$ and $\alpha=(1/24)(a/d)^3$.